

Determining the optimal conditions for the removal of lead ions from aqueous solutions using various biochar samples.

Mustafa Hussein Ali1

Alaa Hasan Fahmi2

1,2Department of Soil Science and Water Recourses, College of Agriculture, University of Diyala, Diyala, Iraq.

1E-mail: mustafahussein989898@gmail.com

Abstract

The aim of this study was to produce biochar from different materials at various temperatures and to determine the optimal conditions for removing heavy metals from aquatic environments. Biochar was prepared through the pyrolysis process of two widely available raw materials in Diyala Governorate, Iraq: palm kernel and sheep manure at temperatures of 300 °C and 700 °C. These were designated as PFB-300, PFB-700, SMB-300, and SMB-700, respectively. The morphological properties of the biochar samples were analyzed using multiple techniques, including Fourier Transform Infrared Spectroscopy (FT-IR), Brunauer-Emmett-Teller (BET) surface area analysis, and Zeta Potential measurement. FT-IR results showed that the biochar contained an abundance of functional groups, while BET analysis revealed that PFB-700 had the highest surface area, followed by SMB-700, PFB-300, and SMB-300, respectively. Zeta Potential tests indicated that the surface charge becomes more negative with increasing production temperature. The samples were applied as adsorbent materials for lead ion adsorption under various conditions, including initial ion concentration (10, 50, 100, 150, 300, 450 ppm), equilibrium time (5, 15, 30, 60, 90, 120 minutes), temperature (298, 308, 318 K), and pH effect (5, 7, 9). The results showed that Pb²⁺ ion adsorption increased significantly in the first few minutes, then slowed down, reaching equilibrium at 30 minutes for PFB-700 and SMB-700, and at 120 minutes for PFB-300 and SMB-300. The rate of Pb²⁺ ion removal increased with temperature, indicating an endothermic adsorption process. Additionally, Pb²⁺ ion removal increased significantly with increasing concentration up to 150 ppm, after which removal efficiency decreased due to the saturation.

Key words: biochar, adsorption, heavy metals, Lead.

Introduction

Pollution is any harmful alteration in the environment resulting from the physical, chemical, or biological side effects of industrial, social, or agricultural human activities. This affects the quality of the environment and poses a threat to humans, animals, plants, and aquatic wildlife [1]. The complexity of the pollution problem increases with the variety and sources of pollutants, due to the excessive use of industries and chemical agriculture in large quantities for different

purposes, such as pesticides, fertilizers, and various types of detergents. Some countries have also contributed to exacerbating the problem by conducting nuclear explosions underground, in deep seas, and on the earth's surface [2]. Among the most dangerous pollutants are heavy metals, which are any metallic elements with a relatively high density exceeding 5 g/cm³. The toxicity of heavy metals varies, as most are considered nutrients at low concentrations and are classified as essential micronutrients for

plants, such as copper (Cu), zinc (Zn), nickel (Ni), and molybdenum (Mo). Conversely, some heavy metals are toxic and hazardous even at low concentrations, such as lead (Pb), cadmium (Cd), arsenic (As), mercury (Hg), and others [3]. Water pollution by heavy metals is a major concern due to their toxicity levels, abundance, environmental stability, and accumulation in water bodies [4]. This pollution causes severe damage to biological systems, especially with lead, cobalt, and cadmium, which accumulate in living organisms and cause various diseases and disorders even at relatively low levels due to their water solubility and non-biodegradability. They can accumulate in the environment and microorganisms, eventually transferring to the human body [5]. Exposure to heavy metal ions, such as lead, cadmium, mercury, and arsenic, even at low concentrations, can negatively affect human health, leading to various types of cancers, neurological and mental issues. Additionally, they hinder plant growth, deform leaves, and reduce fruit production [6]. The growing awareness of current and past environmental issues reflects an urgent need for fundamental reforms to restore and purify the environment and ensure its sustainability. Consequently, various techniques are used in different parts of the world to remove heavy metals, such as chemical precipitation, ion exchange, reverse osmosis, electrochemical treatment, evaporation, and distillation [7]. However, these methods have disadvantages, including incomplete removal, high energy consumption, and the production of toxic substances [8], indicating that they are neither effective nor economical for water environments. Previous studies have recommended adsorption as an effective method for purifying water from heavy metals.

These studies have demonstrated the effectiveness of adsorption in removing heavy metals and highlighted its importance as a reliable purification method. However, they also noted that the effectiveness of adsorption can vary depending on the conditions, materials, and techniques used [9,10,11]. Among the best adsorbent materials is activated carbon, which is effective due to its large surface area and semi-porous structure. However, it is considered unsustainable for several reasons, including its flammability under certain conditions and the potential for severe environmental damage when disposed of improperly [12]. Therefore, it is essential to consider sustainable and environmentally friendly alternatives for use as safe adsorbent materials. Biochar is a safe and effective method for removing pollutants and heavy metals from the environment, as it is a natural, effective, and eco-friendly material. Biochar is produced from organic materials such as wood or animal manure by heating them in the absence of oxygen. Biochar's ability to decompose naturally without leaving harmful residues makes it an effective and sustainable solution for environmental pollutant treatment [12,13]. The chemical and physical properties of biochar are the primary factors that determine its usage. Previous studies have shown that the properties and effectiveness of biochar are influenced by the type of raw material and the temperature used in its production [14]. One of the main challenges in water purification technology is selecting the appropriate adsorbent material, considering production cost, ease of disposal of the spent adsorbent, environmental impact, and adsorption efficiency [15]. Our current study aims to study the impact of the type of raw material (plant residues: palm fronds, and animal residues: sheep manure) and different

temperatures (300 or 700°C) on the chemical and physical properties of biochar. We will apply the biochar samples prepared from palm fronds and sheep manure, treated at different temperatures (300 and 700°C), as adsorbent

Biochar Samples

Samples of palm fronds (PF) and sheep manure (SM) were collected from the farm at Diyala state, Iraq. The two samples were air-dried, then impurities were removed from them and cut into small parts (2 cm³). The prepared samples were placed in ceramic crucibles with a suitable lid and subjected to the furnace (Nabentherm type Furnace 1300°C, 400 V, 50/60 Hz Germany) for pyrolysis at temperatures (300°C and 700°C) for two hours. After pyrolysis, all biochar samples were ground, passed through a 50- μ m sieve as suggested by Fahmi et al. [16], and stored in glass beakers at room temperature before analysis. Biochar derived from palm fronds was then classified as PFB-300 and PFB-700 produced at 300°C and 700°C, respectively. While biochar produced from sheep manure was classified as SMB-300 and SMB-700, produced at 300°C and 700°C, respectively.

Biochar Characterization

Energy-Dispersive X-Ray (EDX) Analysis

The X-ray energy produced by the sample beam's interaction with the electron to

materials for the adsorption of lead ions. We will also determine the optimal conditions for the adsorption process for all biochar surfaces.

determine the chemical composition. This allows the identification and measurement of the chemical elements present in the samples.

Fourier-transform Infrared Spectroscopy

Biochars were analyzed using Fourier transform infrared spectroscopy to identify functional groups. We used a Shimadzu 1800, a Japanese instrument, to analyze spectra in the 400–4000 cm⁻¹ region after pressing samples combined with KBr into translucent sheets.

The Surface Area

of the samples was evaluated by the Brunauer-Emmett-Teller (BET) technique, which uses N₂ adsorption at 77K and using BELSORP MINI II (Japan). Total surface area was determined using the multipoint BET method, while microspore surface area was calculated using the t-plot method. Pore sizes were evaluated using the Barrett-Joyner-Halenda (BJH) method based on adsorption isotherms, with the total pore volume derived from a single N₂ adsorption point at a relative pressure (P/P₀) of 0.99

Ash

Content

By employing the dry combustion method, we were able to ascertain the biochar's ash composition. For this procedure, you'll need to bake 5 grams of biochar at 500 degrees Celsius for 8 hours, let the crucible cool, and then weigh it. To get the ash percentage, which allows for a precise evaluation of the ash content, we subtracted the sample's beginning weight from its end weight in Equation (1) [17.]

$$\text{Ash content(\%)} = (\text{Weight of ash (g)} / (\text{Dry mass of biochar (g)} - \text{Weight of ash (g)})) \times 100\% \quad (1)$$

PH) and Electrical Conductivities (EC(

The pH of the biochar was analyzed following the method presented by [18]. About 4.0 g of biochar was placed with 100 mL of distilled water in a conical flask, covered with glass, and boiled for 5 minutes. After letting it cool, the pH was measured using a pH meter (Bp3001, Germany). To measure electrical conductivity (EC), the biochar was placed in distilled water with a solid-to-liquid ratio of 1,5, shaken for 24 hours, and then the electrical conductivity was measured using an EC meter (HANNA instrument.(

Zeta Potential

to create a suspension with a concentration of 0.5 g L⁻¹, 200 mL of distilled water was added to 0.1 g of finely processed biochar powder in a conical flask. For 12 hours, the flask was mixed by spinning it at 150 revolutions per minute. Next, we used the Malvern Panalytica zeta potential scale to determine the biochar suspension's zeta potential.

Cation exchange

capacity the cation exchange capacity (CEC) of the samples was determined by a compulsive exchange method²³ as simplified by Shen et al.[18.]

adsorption studies

Removal Percentage the percentage removal of lead ions from the solution was calculated using the following equation:

$$\text{Removal \%} = (C_0 - C_e) / C_0 \times 100 \quad (2)$$

where:(C_e): concentration of lead ions after adsorption (ppm),(C₀): initial concentration of lead ions (ppm.(

Contact Times

To determine the equilibrium time for the adsorption process of lead ions on different biochar surfaces (PFB-300, PFB-700, SMB-300, and SMB-700), 0.1g of each surface was placed in volumetric bottles. Then, 40 mL of lead nitrate solution with a concentration of 150 ppm and neutral pH was added to each bottle. These volumetric bottles were then placed in a water bath equipped with a shaker and temperature control, maintaining a temperature of 299 K. The bottles were shaken at 100 rpm. Afterward, the solid material (biochar) was separated from the liquid by filtration at various time intervals (5, 15, 30, 60, 90, and 120 minutes).The filtrate was analyzed to measure the concentration of lead ions using an atomic absorption spectrometer. The percentage removal of ions from the solution

was calculated using equation (2.)

The optimal temperature

to determine the optimal temperature for the adsorption process of lead ions and assess the temperature effects on the equilibrium solution, 0.1g of the studied biochar surfaces were placed in volumetric bottles. Subsequently, 40 mL of lead nitrate solution with a concentration of 150 ppm and neutral pH was added. These volumetric bottles were placed in a water bath and agitated at 100 rpm for the equilibrium time (120 min for PFB-300 and SMB-300). For surfaces PFB-700 and SMB-700, the equilibrium time was 30 min at different temperatures (298, 308, and 318 K). Afterwards, the biochar was separated from the solution by filtration. The final concentration was measured using an atomic absorption spectrometer, and the percentage removal of ions from the solution was calculated using equation (2.)

Concentration Initial

the behavior of biochar surfaces was determined with varying initial concentrations of lead ions by placing 0.1 g of the biochar surfaces studied in volumetric bottles. Subsequently, 40 mL of lead nitrate solution at different concentrations (10, 50, 100, 150, 300, and 450 ppm) with neutral pH was added. These volumetric bottles were placed in a water bath and maintained at the optimal temperature (318 K). The bottles were then agitated at 100 rpm for the equilibrium time (optimal time) for each biochar surface. Afterward, the solid material (biochar) was separated from the liquid by filtration. The final concentration was determined using an atomic absorption spectrometer, and the

percentage removal of lead ions from the solution was calculated using equation (2.)

The optimal Ph

was determined for biochar surfaces in the equilibrium solution by placing 0.1g of biochar surfaces in volumetric bottles. Subsequently, 40 mL of lead nitrate solution at a concentration of 150 ppm was added. The volumetric bottles were then placed in a water bath and maintained at the optimal temperature. The bottles were agitated at 100 rpm for the equilibrium time specific to each biochar surface at different pH levels (5, 7, and 9). After reaching equilibrium, the solid biochar material was separated from the liquid phase by filtration. The final concentration of lead ions in the solution was determined using an atomic absorption spectrometer. The percentage removal of lead ions from the solution was calculated using equation (2.)

Results and discussion

Fourier-transform infrared spectroscopy

It is an analytical technique used to identify the content of materials the chemical group functions by using an infrared spectrum . From the table.1 of biochar FTIR data shows the different peaks of SMB-700 and SMB-300 corresponding to stretching the O-H broad band at 3444 cm⁻¹ in SMB-300, throughout the increasing of temperature to 700oC the stretching O-H band start to slowly diminish. This was expected due to the mass loss during thermal decomposition and gas product evolution [19 .]

The peak 2939 cm⁻¹ in SMB-300 biochar shows sharper peak 2879 cm⁻¹ as the temperature increased in SMB-700 biochar

which belong to the stretching vibration of C-H, the absorption peaks at 1616 cm^{-1} and 1423 cm^{-1} in SMB700 and SMB-300 biochars is attributed to the stretching vibration of C=C and C=O [20]. The peak 1089 cm^{-1} of SMB-300 biochar associated with C-O vibrations in esters and ethers and the same for SMB-700 biochar peak 1035 cm^{-1} [21]. The absorption peak of 873 cm^{-1} in both SHB-300 and SHB-700 biochars is attributed to the bending vibration of C-H on the aromatic ring [19, 20]. FTIR spectrum of PFB-300 biochar shows peaks at 3441 cm^{-1} which obtained to be sharper peak at 3410 cm^{-1} as the temperature increased in PFB-700 attributable to the

stretching O-H possibly from carboxyl, phenol, and alcohol functional groups [22]. We also notice the distinctive C-H stretching vibration of the alkyl structure of aliphatic groups at 2877 cm^{-1} for PFB-700 but not for the PFB-300 [23,24]. The band at 1697-1512 cm^{-1} in both PFB-300 and PFB-700 biochar sample due to the presence of aromatic C=C and C=O stretching vibration represented possible conjugated ketones 1600 cm^{-1} [25,26]. A peak of C-O stretching is also presented in the sample at 1149 cm^{-1} and 1168 cm^{-1} for PFB-300 and PFB-700, respectively [27].

Table (1): shows the group functions of Biochars samples.

Wave number (cm^{-1})	Palm fronds (PFB)		Sheep waste (SMB)		Vibration characteristics
	300 $^{\circ}$ c	700 $^{\circ}$ c	300 $^{\circ}$ c	700 $^{\circ}$ c	
3500-3250	+	+	+	+	O-H stretching
~2880	-	+	-	+	C-H stretching
~1470-1430	+	+	+	+	C-H stretching
1500	-	+	-	+	C=C stretching
3750	-	+	+	+	N-H bend
~1150	+	+	-	-	C-O bend
~1100	-	-	+	+	C-O bend
880-500	-	-	+	+	aromatic ring
1000-625	+	+	-	-	aromatic ring

X-ray spectroscopy (EDX (

The (calcium, potassium, and phosphorus) elements in both biochar samples, PFB-300 and PFB-700, as shown in Table 5 revealed low levels. In contrast, the biochar derived from sheep manure (SMB-300 and SMB-700) showed acceptable levels of elements. Significantly, a decrease in phosphorus levels from 3.24 to 1.24 was observed when the

pyrolysis temperature increased from 300 to 700 degrees. The element content of biochar depends on the nature and quality of the raw materials, as well as the appropriate pyrolysis conditions (see Fig.1). High temperatures during pyrolysis lead to the volatilization of some elements, which is consistent with previous studies [28,29].

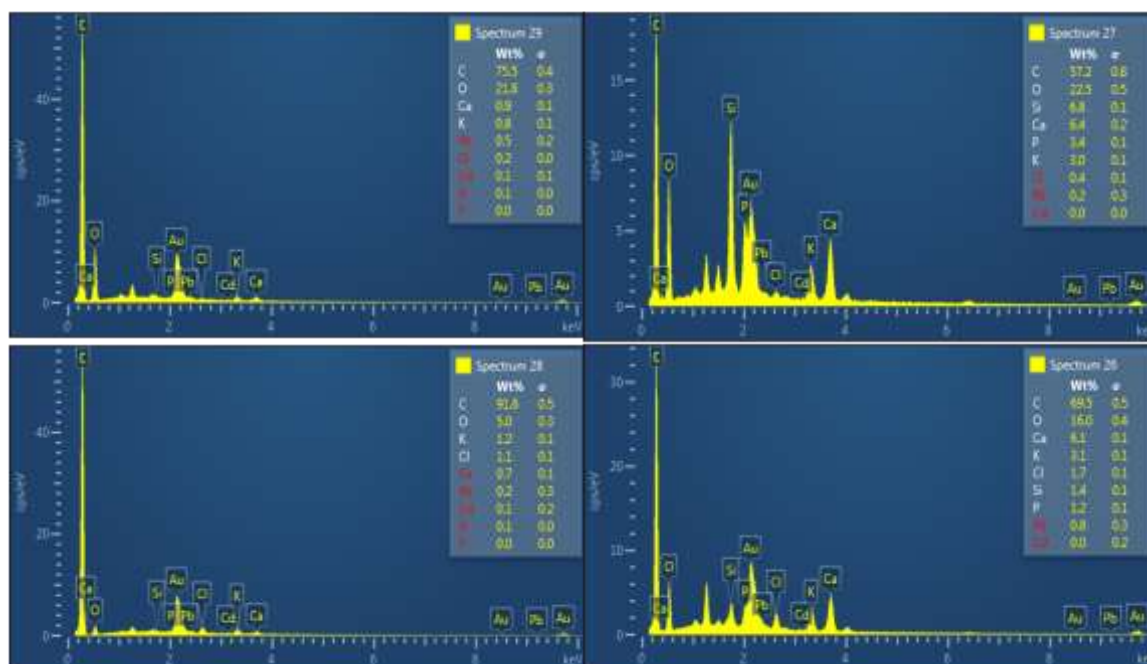


Fig.(1).EDX spectra For PFB and SMB at 300°C and 700 °C. BET surface area analysis.

The surface area of biochar samples was measured using the BET technique, and the results showed variation in surface area values: 20.61 m² g⁻¹ for PFB-300, 247.7 m² g⁻¹ for PFB-700, 17.07 m² g⁻¹ for SMB-300, and 89.89 m² g⁻¹ for SMB-700, as listed in Table (2). The results indicate that the highest surface area was for the PFB-700 sample, and there was an observed increase in surface area with the rise in pyrolysis temperature. This is attributed to the effect of high heat in fragmenting particles and altering the surface structure, increasing the number of pores, leading to the spread of cracks and pits, and thus these factors collectively or individually contribute to the increase in surface area.[26] reached similar conclusions, indicating that raising the biochar production temperature from seaweed from 300 °C to 400 °C resulted in significant changes in structural and chemical composition, as well as an increase in surface area and porosity.

Regarding the total pore volume, it showed similar behavior to the surface area with rising temperature. The total pore volume for PFB-300, PFB-700, SMB-300, and SMB-700 was 0.03 cm³ g⁻¹, 0.18 cm³ g⁻¹, 0.06 cm³ g⁻¹, and 0.14 cm³ g⁻¹, respectively, as shown in Table (2). The increase in total pore volume is attributed to the same reasons that led to the increase in surface area, and the difference in raw material had a negligible effect. Our results are consistent with Tsai et al. [27], who observed a significant increase in total pore volume from 0.0005 cm³ g⁻¹ to 0.153 cm³ g⁻¹ with an increase in temperature from 400 °C to 800 °C, attributing this to the increased formation of nanopores and fine structures on the biochar surface. These findings agree with FESEM measurements that confirmed surface development, increased surface area, and pore density in PFB-700 and SMB-700 compared to PFB-300 and SMB-300, making them prime candidates for applications in water and

soil purification through the adsorption of cationic chemicals and organic pollutants [25.]

Ash Content

The ash content in the biochar samples was estimated using equation (1), and it was found that the biochar samples from palm charcoal contain higher ash percentages: 55.14%, 73.7%, 38.42%, and 62.28% for PFB-300, PFB-700, SMB-300, and SMB-700, respectively, as listed in Table (2). The high ash content in PFB-300 and PFB-700 samples is attributed to their mineral composition, which includes higher percentages of inorganic minerals such as silica, calcium, and magnesium. When the raw material is thermally processed, these minerals remain as ash.

Additionally, there is an observed increase in ash content in all biochar samples with the rise in pyrolysis temperature. This is due to the decomposition of organic materials into gases and volatile substances, reducing the combustible organic portion and leaving the inorganic minerals as ash. Research by Andelini et al. [30] found similar results, with ash content increasing from 8.36% to 9.6% when the pyrolysis temperature was raised from 400 °C to 600 °C. Tomczyk et al. [31] also noted that biochar produced from animal waste has lower ash and carbon content compared to biochar produced from crop residues and wood biomass. They indicated that the variation in ash content and some physical and chemical properties is due to differences in moisture content, organic materials, and lignocellulosic compounds in the raw materials used.

pH we observe that biochar samples produced at 300 °C have lower pH values compared to

other samples, which could be attributed to the presence of larger amounts of carboxylic and phenolic acid groups, as documented by FT-IR analysis. On the other hand, samples produced at 700 °C show higher surface pH, attributed to the effect of temperature on increasing the carbonization of samples and the ash content, which is rich in mineral elements such as potassium, sodium, calcium, magnesium, and minerals like carbonates that impart alkaline properties. Zhu et al. [32] obtained similar results, where pH values increased from 7.4 to 11.6 as the temperature rose from 300 °C to 500 °C, coinciding with an increase in ash content. Das et al. [33] also found that the highest pH was for biochar produced at 400 °C, which decreased with increasing temperature.

The results also indicate that biochar derived from sheep manure has higher pH values at the specified temperatures, as shown in Table (2). This difference is attributed to the chemical composition of the ash. It is noteworthy that the acidity of biochar affects its efficiency in absorbing heavy metals, with alkaline biochar being more effective compared to acidic biochar. This is consistent with the findings of Tag et al. [34] who studied four types of raw materials: agricultural waste, industrial waste, animal waste, and algae.

Electrical Conductivity

The results indicate an increase in electrical conductivity with rising temperature, which is attributed to the same reasons that lead to increased ash content and higher pH, due to the interrelationship between these factors. A study by Almutairi et al. [35] confirmed this correlation across nine types of waste,

including palm leaves, wood, and animal waste .

Electrical Charges

We observe that the values of electric charges decrease (become more negative) with an increase in temperature from 300 °C to 700 °, as shown in Table (2). A significant difference in charge values was noted between PFB-300 and PFB-700, which could be attributed to the emergence of active groups not present in PFB-300, as shown in the FT-IR analysis in Table (1). Ding et al. [36] reached similar results to our study, showing a decrease in electric charge values (increase in negative values) for biochar produced from oak, from -27.5 mV to -32.4 mV, with an increase in temperature from 350 °C to 650 °C. However, our results differ from the study by Suliman [37] where electric charge values increased with the rise in production temperature for biochar from wood and organic waste. In our view, this difference may be due to the removal of oxidized functional groups from the biochar surface, which are responsible for the surface charge, unlike in our study.

It is also worth noting that the abundance of negative charges on the surfaces of the studied biochar makes them more capable of interacting with positively charged ions such as lead. As a result, the more negative biochar appears to be more suitable as an adsorbent material .

CEC We observe an increase in the biochar's ability to adsorb and exchange positively charged ions with rising temperatures, as shown in Table (2). This may be attributed to the abundance of oxidized functional groups (O-H, C-O, C=O) and positively charged ions. It should be noted that CEC represents the cations held by negative charges, which can indicate the total negative charges on the surface, aligning with the zeta potential analysis. The general increase in cation exchange capacity (CEC) with rising temperature is consistent with Das et al. [33], who studied the effect of raw materials (grasses, trees, and crop residues) and temperature (300, 500, 700 °C) on the properties of the produced biochar. They found an increase in carbon content and cation exchange capacity

Table (2): The physicochemical characteristics of the SMBs and PFBs.

Parameters	SMB-300	SMB-700
Ash content (%)	38.42	62.28
surface area ($\text{m}^2 \text{g}^{-1}$)	17.07	89.89
Total pore volume ($\text{cm}^3 \text{g}^{-1}$)	0.06	0.14
pH	7.82	10.7
EC (dS m^{-1})	7.6	8.2
Electric Charges (mv)	-6.12	-8.01
CEC $\text{cmol}^{(+)}\text{kg}^{-1}$ by (BaCl_2)	36.8	47.80
Parameters	PFB-300	PFB-700
Ash content (%)	55.14	73.7
surface area ($\text{m}^2 \text{g}^{-1}$)	20.61	247.77
Total pore volume ($\text{cm}^3 \text{g}^{-1}$)	0.03	0.18
pH	6.44	9.72
EC (dS m^{-1})	6.41	16.3
Electric Charges (mv)	-2.96	-8.39
CEC $\text{cmol}^{(+)}\text{kg}^{-1}$ by (BaCl_2)	27.1	52.31

adsorption studies

Contact Times

The results of testing the contact times between different biochar surfaces and lead ion solution indicated that the equilibrium time for both PFB-300 and SMB-300 was 120 minutes, whereas for both PFB-700 and SMB-700, it was 30 minutes, as shown in Table(3). It is noted that the percentage removal of lead ions increases significantly in the initial minutes of the adsorption process and then slows down noticeably. This suggests that most active sites become saturated with lead ions in the early minutes, and upon reaching equilibrium, the adsorption rate ceases due to complete saturation of reactive sites on the surface, making the increase in time after equilibrium less effective. Furthermore, the results showed that the percentage removal of lead ions on PFB-700 and SMB-700 surfaces

was higher than on SMB-300 and PFB-300 surfaces. Several factors contribute to this, including larger surface area, abundant pores, negative charge, and positive ion exchange capacity, as evidenced by previous tests. Our study results align with previous studies such as those by Hummadi and Lee et al. [38,39] where they found that the highest capacity for heavy metal adsorption occurs at equilibrium, after which the adsorption efficiency becomes constant with increasing time. They explained that this phenomenon is due to the saturation of the adsorbent material with heavy metals. These findings are supported by another study conducted by Abyaneh et al. [40], who prepared biochar at different temperatures (400 °C, 500 °C, and 700 °C) and tested its ability to remove lead from industrial

wastewater in Tehran, Iran. They found that biochar prepared at 700 °C was the most effective, attributing this to increased thermal

decomposition enhancing surface development and forming a more porous structure

Table (3): The percentages of lead ion removal using biochar surfaces at different contact times.

Time (min)	C ₀ (PPM)	PFB-300		SMB-300	
		Ce (ppm)	R%	Ce (ppm)	R%
5	150	24.76	83.48	39.36	73.75
15		14.31	90.45	29.14	80.57
30		10.58	92.94	24.91	83.38
60		3.63	97.57	19.85	86.76
90		3.14	97.90	23.21	84.52
120		0.44	99.70	14.48	90.34
Time (min)		PFB-700		SMB-700	
		Ce (ppm)	R%	Ce (ppm)	R%
5		0.086	99.94	149.82	99.88
15		0.086	99.94	149.47	99.65
30		0	100	150	100
60		0.330	99.77	150	100
90	0.043	99.97	148.85	99.23	
120	0	100	148.15	98.77	

The optimal temperature

The results of temperature impact tests on the adsorption process of lead ions on biochar surfaces, as shown in Table (4), indicated that the percentage removal of lead ions increases with higher temperatures. This suggests that the adsorption process is heat-dependent, indicating that the selectivity of lead ions on biochar surfaces increases with temperature. Additionally, heat increases the kinetic energy of lead ion particles, allowing them to diffuse more effectively into the pores of biochar. Furthermore, it was observed that both PFB-700 and SMB-700 exhibited higher efficiency in lead ion adsorption rates, attributed to their distinct properties of high porosity, abundant pores, and negative charges as previously mentioned. These properties enable these

surfaces to remove higher percentages of lead ions, a finding supported by Energy Dispersive X-ray Spectroscopy (EDX) results, showing higher lead content on these surfaces. Our findings are consistent with a study by Shen et al. [41], where rice straw-derived biochar produced at different temperatures (300 °C, 500 °C, and 700 °C) demonstrated that biochar produced at higher temperatures had a higher capacity for lead ion adsorption and removal due to its increased surface area. Similarly, Sun et al. [42] concluded in their study testing different temperatures (303 K, 308 K, 313 K, and 330 K) on equilibrium solutions that biochar exhibited higher pollutant removal capabilities at higher temperatures, reflecting its heat-dependent nature

Table (4): The percentages of lead ion removal using biochar surfaces at different temperatures.

temperature (min)	C ₀ (PPM)	PFB-300		SMB-300	
		Ce (ppm)	R%	Ce (ppm)	R%
299	150	1.218	99.18	14.52	90.31
309		0.751	99.49	2.76	98.15
319		1.218	99.52	0.968	99.35
temperature (min)		PFB-700		SMB-700	
		Ce (ppm)	R%	Ce (ppm)	R%
299		0.762	99.49	1.429	99.04
309		0.260	99.82	0.065	99.95
319		0	100	0.329	100

Concentration Initial

The results of testing the initial ion concentration's effect on lead ion adsorption on biochar surfaces, as illustrated in Table (5), showed that the percentage removal of lead ions increases with higher concentrations of lead ions (Pb²⁺). This is attributed to an increased number of collisions between the metal ion and the biochar surface, enhancing interaction with available active sites and facilitating ion transfer into the inner pores. However, as the concentration of lead ions increases to 300 ppm and 450 ppm, the percentage removal decreases, as indicated in Table (5). This is due to saturation of active sites and pores on the surface. Nevertheless, the removal efficiency of lead ions on PFB-700 and SMB-700 surfaces was significantly

higher than on other surfaces, thanks to their distinctive properties such as high surface area, abundant pores, high electric charge, and higher ion exchange capacity. Our findings are consistent with a study by Abdelhafez and Li [43], where biochar derived from orange peels and sugarcane bagasse at 500 °C was used to remove lead ions. The study examined various factors, including initial lead ion concentration, and found that the biochar's adsorption capacity increases with higher initial ion concentrations due to increased ion driving forces. However, the results showed that the increase becomes insignificant beyond a concentration of 85 ppm, attributed to saturation of active sites on the biochar surface.

Table (5): The percentages of lead ion removal using biochar surfaces at different ion concentration levels.

C _o (PPM)	PFB-300		SMB-300	
	Ce (ppm)	R%	Ce (ppm)	R%
10	0.2004	99.5	0.412	95.87
50	0.565	98.96	0.542	98.91
100	0.483	99.51	1.403	98.59
150	0.751	99.49	0.968	99.35
300	51.937	82.68	39.085	86.97
450	138.03	69.32	90.503	79.88
C _o (PPM)	PFB-700		SMB-700	
	Ce (ppm)	R%	Ce (ppm)	R%
10	0.224	97.75	0.212	97.87
50	0.224	99.55	0.1650	99.66
100	0.318	99.68	0.565	99.43
150	0.362	99.96	0.065	99.95
300	0.119	99.75	1.013	99.66
450	1.379	99.69	4.952	98.89

The optimal pH

The test results on pH values of the solution showed variability in the percentage removal of lead ions using different biochar samples, as depicted in Table (6). The highest removal was observed at pH 7, compared to pH 5 and pH 9. This can be attributed to the high concentration of hydrogen ions (H^+) at low pH, leading to the presence of hydronium ions (H_3O^+) surrounding the biochar surface. This reduces the interaction of lead ions with binding sites on the biochar surface due to repulsive forces. Additionally, the smaller size of hydrogen ions allows them to permeate into the gaps and pores of the biochar, occupying them and preventing larger lead ions from entering, thereby reducing the biochar's ability to remove lead ions in acidic environments as shown in Table (6). Furthermore, pH plays a crucial role in determining surface charge, where biochar surfaces tend to acquire a

positive charge in acidic environments, while they are negatively charged in neutral and alkaline conditions. Our findings align with a study conducted by Abyaneh et al. [40], which found maximum removal efficiency at pH 7 using wood waste-derived biochar. Similarly, a study by Wang et al. [44] demonstrated that cadmium removal efficiency using corn stalk-derived biochar increased from 37.3% to 96.7% as pH increased from 2 to 6.5. At pH 9, where hydroxide ions (OH^-) are abundant in the aqueous solution, lead may precipitate as $Pb(OH)_2$ and not interact with the biochar surface, consistent with findings from Yang et al. [45]. They indicated that lead ion removal using corn stalk-derived biochar at pH greater than 7 involved not only adsorption but also precipitation processes. Therefore, pH 7 is considered most suitable for lead ion adsorption in our current study.

Table (6): The percentages of lead ion removal using biochar surfaces at different pH levels.

pH	C _o (PPM)	PFB-300		SMB-300	
		Ce (ppm)	R%	Ce (ppm)	R%
5	150	40.441	73.03	23.22	84.51
7		0.751	99.49	0.577	99.61
9		0.848	99.43	0.968	99.35
pH		PFB-700		SMB-700	
		Ce (ppm)	R%	Ce (ppm)	R%
5		0.565	99.62	0.683	99.54
7		0.362	99.75	0.065	99.95
9		0.589	99.60	0.436	99.70

Conclusions

This study concluded that the pyrolysis temperature affects both surface chemistry and physical properties. Pyrolysis of sheep manure produced biochar rich in stable aromatic carbon structures and essential inorganic minerals. Raising the pyrolysis temperature to 700°C enhanced the development of pores, surface area and negative charge, making biochar adept at purifying water and soil by adsorbing cationic chemicals pollutants. The adsorption process is simple, low-cost, and highly effective in removing lead ions using biochar produced from palm fronds and sheep manure. The equilibrium time for the

adsorption of lead ions (Pb²⁺) on PFB-700 and SMB-700 was achieved in 30 minutes, while it was achieved on PFB-300 and SMB-300 in 120 minutes. The lead ion removal rate by biochar surfaces increases with temperature, with the optimal temperature being 318 K. Lead ion removal is preferred in moderately acidic environments. Biochar produced from palm fronds at 700°C showed the highest lead ion removal rate, followed by biochar from sheep manure at the same temperature, indicating the effectiveness of high temperatures in activating biochar surfaces

References

- MaryGurrie, . Water Quality in 2020: An Indicators Report. The Environmental Protection Agency (EPA), 2021.
- [2] Inyinbor Adejumo, A., Adebisin Babatunde, O., Oluyori Abimbola, P., Adelani Akande Tabitha, A., Dada Adewumi, O., and Oreofe Toyin, A. (2018). Water pollution: effects, prevention, and climatic impact. *Water challenges of an urbanizing world*, 33, 33-47..
- [1] [3] Zhu, X., Chen, B., Zhu, L., and Xing, B. (2017). Effects and mechanisms of biochar-microbe interactions in soil improvement and pollution remediation: a review. *Environmental pollution*, 227, 98-115.
- [4] Eko Bessa, A. Z., Nguetchoua, G., Kwewouo Janpou, A., El-Amier, Y. A., Njike Njome Mbella Nguetnga, O. A., Kankeu Kayou, U. R., ... & Armstrong-Altrin, J. S.

(2021). Heavy metal contamination and its ecological risks in the beach sediments along the Atlantic Ocean (Limbe coastal fringes, Cameroon). *Earth Systems and Environment*, 5, 433-444.

[5] Kavitha, B., Reddy, P. V. L., Kim, B., Lee, S. S., Pandey, S. K., and Kim, K. H. (2018). Benefits and limitations of biochar amendment in agricultural soils: A review. *Journal of environmental management*, 227, 146-154 .

[6] Xu, X., Schierz, A., Xu, N., and Cao, X. (2016). Comparison of the characteristics and mechanisms of Hg (II) sorption by biochars and activated carbon. *Journal of colloid and interface science*, 463, 55-60.

[7] Vunain, E., Masoamphambe, E. F., Mpeketula, P. M. G., Monjerezi, M., and Etale, A. (2019). Evaluation of coagulating efficiency and water borne pathogens reduction capacity of *Moringa oleifera* seed powder for treatment of domestic wastewater from Zomba, Malawi. *Journal of Environmental Chemical Engineering*, 7(3), 103118.

[8] Eccles, H. (1999). Treatment of metal-contaminated wastes: why select a biological process? *Trends in biotechnology*, 17(12), 462-465 .

[9] Bashir, A., Malik, L. A., Ahad, S., Manzoor, T., Bhat, M. A., Dar, G., and Pandith, A. H. (2019). Removal of heavy metal ions from aqueous system by ion-exchange and biosorption methods. *Environmental Chemistry Letters*, 17, 729-754 .

[10] Vázquez-Guerrero, A., Cortés-Martínez, R., Alfaro-Cuevas-Villanueva, R., Rivera-Muñoz, E. M., and Huirache-Acuña, R. (2021). Cd (II) and Pb (II) adsorption using a composite obtained from *moringa oleifera*

lam. Cellulose nanofibrils impregnated with iron nanoparticles. *Water*, 13(1), 89 .

[11] Joshi, S., Singh, H., Sharma, S., Barman, P., Saini, A., and Verma, G. (2021). Synthesis and characterization of graphene oxide-bovine serum albumin conjugate membrane for adsorptive removal of Cobalt (II) from water. *International Journal of Environmental Science and Technology*, 1-14 .

[12] Shakoor, M. B., Ali, S., Rizwan, M., Abbas, F., Bibi, I., Riaz, M., Khalil, U., Niazi, N. K., and Rinklebe, J. (2020). A review of biochar-based sorbents for separation of heavy metals from water. *International Journal of Phytoremediation*, 22(2), 111-126.

[13] Khadem, M., Husni Ibrahim, A., Mokashi, I., Hasan Fahmi, A., Noeman Taqui, S., Mohanavel, V., ... and Syed, A. A. (2023). Removal of heavy metals from wastewater using low-cost biochar prepared from jackfruit seed waste. *Biomass Conversion and Biorefinery*, 13(16), 14447-14456.

[14] Wang, L., Deng, J., Yang, X., Hou, R., and Hou, D. (2023). Role of biochar toward carbon neutrality. *Carbon Research*, 2(1), 2.

[15] Yerli, C. (2023). The Effects of Biochar Pyrolyzed at Varying Temperatures and Different Water Types on the Properties of Lettuce and Soil. *Water, Air, and Soil Pollution*, 234(8), 552.

[16] Fahmi, A. H., Jol, H., and Singh, D. (2018). Physical modification of biochar to expose the inner pores and their functional groups to enhance lead adsorption. *RSC advances*, 8(67), 38270-38280. [16] SPSS Inc. 2011. Statistical Package for social Sci version 20 for windows LEAD Technologies. Inc. USA .

[17] Chen, B., Zhou, D., & Zhu, L. (2008). Transitional adsorption and partition of nonpolar and polar aromatic contaminants by biochars of pine needles with different

pyrolytic temperatures. *Environmental science & technology*, 42(14), 5137-5143.

[18] Sun, H., Zhang, Y., & Zhang, W. (2013). Biochar and environment. In, Chemical Industry Press Beijing [in Chinese.]

[19] Dilekoğlu, M. F. (2022). Malachite green adsorption from aqueous solutions onto biochar derived from sheep manure, adsorption kinetics, isotherm, thermodynamic, and mechanism. *International Journal of Phytoremediation*, 24(4), 436-446..

[20] Chen, J., Li, S., Huang, Q., Liu, H., Sun, J., Zhang, Y., & Lu, Y. (2022). Preparation of sheep manure biochar and its enhancement effect on wastewater treatment performance of CRI systems. *MATEC Web of Conferences*,

[21] Boostani, H. R., Najafi-Ghiri, M., Hardie, A. G., & Khalili, D. (2019). Comparison of Pb stabilization in a contaminated calcareous soil by application of vermicompost and sheep manure and their biochars produced at two temperatures. *Applied Geochemistry*, 102, 121-128 .

[22] Azeez, L., Oyefunke, O., Oyedeji, A. O., Agbaogun, B. K., Busari, H. K., Adejumo, A. L., Agbaje, W. B., Adeleke, A. E., & Samuel, A. O. (2024). Facile removal of rhodamine B and metronidazole with mesoporous biochar prepared from palm tree biomass, adsorption studies, reusability, and mechanisms. *Water Practice & Technology*, wpt2024049..

[23] Alwan, Q. H., Rahman, A. M., Salman, M. H., & Ali, Z. H. (2015). Characterization of Biochar Produced from IRAQI Palm Fronds by Thermal Pyrolysis. *Al-Khwarizmi Engineering Journal*, 11(2), 92-102.

[24] Feng, Y., Zhao, D., Qiu, S., He, Q., Luo, Y., Zhang, K., Shen, S., & Wang, F. (2021). Adsorption of phosphate in aqueous phase by biochar prepared from sheep manure and modified by oyster shells. *ACS omega*, 6(48), 33046-33056.

[25] Janu, R., Mrlik, V., Ribitsch, D., Hofman, J., Sedláček, P., Bielská, L., & Soja, G. (2021). Biochar surface functional groups as affected by biomass feedstock, biochar composition and pyrolysis temperature. *Carbon Resources Conversion*, 4, 36-46 ..

[26] Sizirici, B., Fseha, Y. H., Yildiz, I., Delclos, T., & Khaleel, A. (2021). The effect of pyrolysis temperature and feedstock on date palm waste derived biochar to remove single and multi-metals in aqueous solutions. *Sustainable Environment Research*, 31, 1-16

[27] Salem, I. B., Saleh, M. B., Iqbal, J., El Gamal, M., & Hameed, S. (2021). Date palm waste pyrolysis into biochar for carbon dioxide adsorption. *Energy Reports*, 7, 152-159..

[28] Tripathi, M., Sahu, J. N., & Ganesan, P. (2016). Effect of process parameters on production of biochar from biomass waste through pyrolysis, A review. *Renewable and sustainable energy reviews*, 55, 467-481.

[29] Mohan, D., Sarswat, A., Ok, Y. S., & Pittman Jr, C. U. (2014). Organic and inorganic contaminants removal from water with biochar, a renewable, low cost and sustainable adsorbent—a critical review. *Bioresource technology*, 160, 191-202.

[30] Anđelini, D., Cvitan, D., Prelac, M., Pasković, I., Černe, M., Nemet, I., ... and Palčić, I. (2023). Biochar from Grapevine-Pruning Residues Is Affected by Grapevine Rootstock and Pyrolysis Temperature. *Sustainability*, 15(6), 4851..

[31] Tomczyk, A., Sokołowska, Z., and Boguta, P. (2020). Biochar physicochemical properties: pyrolysis temperature and feedstock kind effects. *Reviews in Environmental Science and Bio/Technology*, 19(1), 191-215.

- [32] Zhu, X., Chen, B., Zhu, L., and Xing, B. (2017). Effects and mechanisms of biochar-microbe interactions in soil improvement and pollution remediation: a review. *Environmental pollution*, 227, 98-115 .
- [33] Das, S. K., Ghosh, G. K., Avasthe, R. K., and Sinha, K. (2021). Compositional heterogeneity of different biochar: effect of pyrolysis temperature and feedstocks. *Journal of Environmental Management*, 278, 111501..
- [34] Tag, A. T., Duman, G., Ucar, S., and Yanik, J. (2016). Effects of feedstock type and pyrolysis temperature on potential applications of biochar. *Journal of Analytical and Applied Pyrolysis*, 120, 200-206
- [35] Almutairi, A. A., Ahmad, M., Rafique, M. I., and Al-Wabel, M. I. (2023). Variations in composition and stability of biochars derived from different feedstock types at varying pyrolysis temperature. *Journal of the Saudi Society of Agricultural Sciences*, 22(1), 25-34.
- [36] Ding, Z., Wan, Y., Hu, X., Wang, S., Zimmerman, A. R., and Gao, B. (2016). Sorption of lead and methylene blue onto hickory biochars from different pyrolysis temperatures: importance of physicochemical properties. *Journal of Industrial and Engineering Chemistry*, 37, 261-267 .
- [37] W.Suliman. TOWARD AN UNDERSTANDING OF THE ROLE OF BIOCHAR AS AN AGRO-ENVIRONMENTAL TOOL: POTENTIAL FOR CONTROL WATER RELEASE, BACTERIAL RETENTION, AND GREENHOUSE GAS EMISSIONS. *Research Exchange*, 2015 .
- [38] Hummadi, K. K. (2021). Optimal operating conditions for adsorption of heavy metals from an aqueous solution by an agriculture waste. *Iraqi Journal of Chemical and Petroleum Engineering*, 22(2), 27-35.
- [39] Lee, X. J., Lee, L. Y., Gan, S., Thangalazhy-Gopakumar, S., & Ng, H. K. (2017). Biochar potential evaluation of palm oil wastes through slow pyrolysis: thermochemical characterization and pyrolytic kinetic studies. *Bioresource technology*, 236, 155-163.
- [40] Rabiee Abyaneh, M., Nabi Bidhendi, G., & Daryabeigi Zand, A. (2024). Pb (II), Cd (II), and Mn (II) adsorption onto pruning-derived biochar: physicochemical characterization, modeling and application in real landfill leachate. *Scientific Reports*, 14(1), 3426.
- [41] Shen, Z., Hou, D., Jin, F., Shi, J., Fan, X., Tsang, D. C., & Alessi, D. S. (2019). Effect of production temperature on lead removal mechanisms by rice straw biochars. *Science of the Total Environment*, 655, 751-758.
- [42] Sun, L., Chen, D., Wan, S., and Yu, Z. (2018). Adsorption studies of dimetridazole and metronidazole onto biochar derived from sugarcane bagasse: kinetic, equilibrium, and mechanisms. *Journal of Polymers and the Environment*, 26, 765-777.
- [43] Abdelhafez, A. A., & Li, J. (2016). Removal of Pb (II) from aqueous solution by using biochars derived from sugar cane bagasse and orange peel. *Journal of the Taiwan Institute of Chemical Engineers*, 61, 367-375.
- [44] Wang, H., Zhang, M., and Lv, Q. (2019). Influence of pyrolysis temperature on cadmium removal capacity and mechanism by maize straw and platanus leaves biochars. *International Journal of Environmental Research and Public Health*, 16(5), 845.
- [45] Yang, W., Lu, C., Liang, B., Yin, C., Lei, G., Wang, B., ... and Jing, Y. (2023).

Removal of Pb (II) from Aqueous Solution
and Adsorption Kinetics of Corn Stalk

Biochar. Separations, 10(8), 438.